СООБЩЕНИЯ
ОБЪЕДИНЕННОГО
ИНСТИТУТА
ЯДЕРНЫХ
ИССЛЕДОВАНИЙ

ДУБНА

E1 - 8092

B.S.Aladashvili, B.Badełek, V.V.Glagolev,
R.M.Lebedev, J.Nassalski, M.S.Nioradze, I.S.Saitov,
A.Sandacz, T.Siemiarczuk, J.Stepaniak,
V.N.Streltsov, P.Zielinski

CHARGE EXCHANGE IN THE DEUTERON BREAK-UP AT AN INCIDENT DEUTERON MOMENTUM OF 3.3 GEV/C

1974

ЛАБОРАТОРИЯ ВЫСОКИХ ЭНЕРГИЙ

E1 - 8092

B.S.Aladashvili, B.Badełek,[2] V.V.Glagolev,
R.M.Lebedev, J.Nassalski,[2] M.S.Nioradze, I.S.Saitov,
A.Sandacz,[1] T.Siemiarczuk,[1] J.Stepaniak,[1]
V.N.Streltsov, P.Zielinski[2]

CHARGE EXCHANGE IN THE DEUTERON BREAK-UP AT AN INCIDENT DEUTERON MOMENTUM OF 3.3 GEV/C

Dubna - Warsaw Collaboration

[1] Institute of Experimental Physics, Warsaw University.
[2] Institute of Nuclear Research, Warsaw.

Аладашвили Б.С., Бадэлэк Б., Глаголев В.В.,
Лебедев Р.М., Нассальски Я., Ниорадзе М.С.,
Саитов И.С., Сандач А., Семярчук Т.,
Степаняк И., Стрельцов В.Н., Зелински П.

E1 - 8092

Перезарядка в реакции с развалом дейтрона при импульсе падающего дейтрона 3,3 ГэВ/с

Изучалась перезарядка в реакции $dp \to ppn$ при импульсе дейтрона 3,33 ГэВ/с в 1-метровой водородной пузырьковой камере. Оценен вклад не зависящей от спина амплитуды в реакцию перезарядки $np \to pn$ для малых значений $|t|$.

Обсуждены различные механизмы, играющие роль в рассматриваемом процессе.

Сообщение Объединенного института ядерных исследований
Дубна, 1974

Aladashvili B.S., Badełek B., Glagolev V.V.,
Lebedev R.M., Nassalski J., Nioradze M.S.,
Saitov I.S., Sandacz A., Siemiarczuk T.,
Stepaniak J., Streltsov V.N., Zielinski P.

E1 - 8092

Charge Exchange in the Deuteron Break-Up at an Indicent Deuteron Momentum of 3.3 GeV/c

The charge exchange deuteron break-up $dp \to ppn$ is studied at a 3.33 GeV/c deuteron momentum in the 1 m hydrogen bubble chamber.

The contribution of the spin-independent amplitude to the $np \to pn$ charge exchange reaction for low t-values was estimated.

Various mechanisms playing a role in the considered process are discussed.

Communications of the Joint Institute for Nuclear Research.
Dubna, 1974

1. Introduction

In the last years various reactions of high energy particles with deuterons have been extensively studied [1,2] but still there is no experimental data on the charge exchange in the deuteron break-up reaction $pd \to npp$ at the momentum exceeding 1 GeV/c. This is mainly caused by losses of slow protons when a proton beam and a deuteron target are used. The use of the deuteron beam allows one to overcome this difficulty and provides an almost unbiased sample of the $pd \to npp$ reaction.

The are two aims in our study. The first one is an analysis of the following nuclear effects which appear in the nucleon-deuteron interaction: double scattering, final state interaction and intermediate isobar states.

The second purpose is an extraction of information on the elementary $np \to pn$ process. The existing data on this reaction are so far very poor and concern mainly the $\frac{d\sigma}{dt}$ distribution. As a consequence of the definite isotopic spin of the two protons, a study of the symmetry of the spatial part of their wave function in the $pd \to npp$ reaction may give information on the spin structure of the elementary amplitude. A study of the $\frac{d\sigma}{dt}$ differential cross section allows the estimation of the spin-independent contribution to the $np \to pn$ reaction amplitude.

2. Experimental Procedure

The experiment was performed at the JINR proton synchrotron using the 1 m hydrogen bubble chamber exposed to the deuteron beam at a 3.33 ±0.08 GeV/c momentum. About 170 thousand pictures were taken. The admixture of protons in the beam was 9 ± 3%. The details of the experiment and some preliminary results can be found in ref. /3/.

The double scanning was done for a quarter of the number of the pictures taken, and about 20 thousand two-prong events lying in a fiducial region of the chamber were found. The use of the deuteron beam, which provides low systematic losses in all break-up channels, is particularly favourable for the selection of the charge exchange sample. These events correspond mostly to two-prong interactions with two fast protons in the laboratory system.

The conventional THRESH-GRIND system was used in the data analysis. 8358 two-prong events were fitted to the reaction

$$dp \to ppn \qquad (1)$$

and were consistent with the expected bubble density. One event in the analysed film sample corresponds to the cross section 4.30 μb.

About 85% of the events fitting the reaction (1) are unambiguous. The remaining events are ambiguous mainly due to the proton admixture in the beam. The contribution of the p−p interaction to the reaction (1) was estimated to be 0.7%. This estimate was done using the program FAKE with the angular distribution of the secondaries in the nucleon-nucleon interaction, the cross section for the p−p interactions and the amount of the proton admixture in the beam. The number of events fitting simultaneously the other channels is negligible. It was also found using FAKE that ~4% of the $dp \to ppn$ events had gone from the break-up sample fitting the pp channels with at least three times higher probability $P(\chi^2)$.

The measurement error of the proton momentum at 1.5 GeV/c is equal to ~ 30 MeV/c; this gives an error of ~ 15 MeV/c in the deuteron rest system. The error for a neutral particle momentum was estimated to be about 2.5 times higher.

3. Definition of the Charge Exchange Event

In the study of high energy nuclear reactions, the coordinate system in which the nucleus is at rest is customarily used. For that reason all physical quantities will now be given in the deuteron rest system.

In the elementary $pn \to np$ interaction, the charge exchange reaction is defined as an event in which the proton is scattered backward in the center-of-mass system of the colliding nucleons. At our energy this corresponds to the

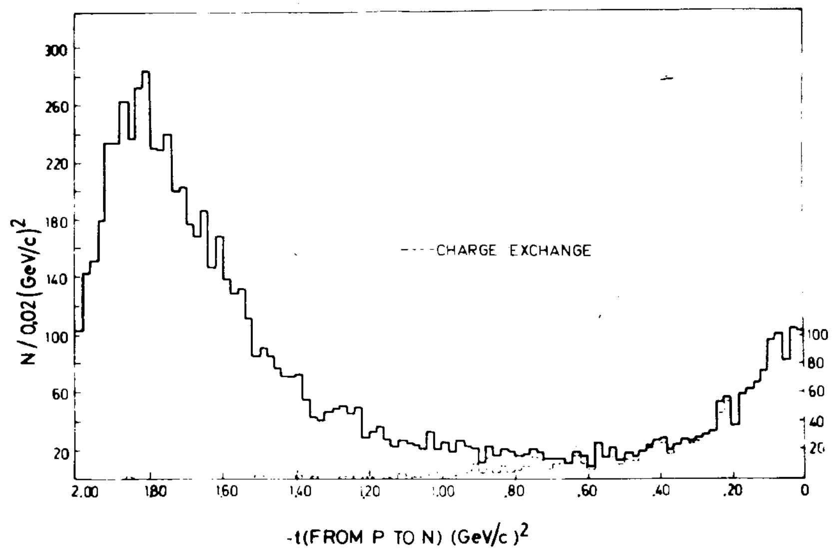

Fig. 1. The $d\sigma/dt$ distribution for all deuteron break-up events; t is the four-momentum transfer from the target proton to the neutron. The dotted line corresponds to the events with the neutron momentum higher than the momentum of any proton in the charge-exchange event.

four-momentum transfer from a proton to a neutron less than 0.91 $(GeV/c)^2$.

For a proton-deuteron interaction this definition does not hold since for high t -transfers the impulse model is not a good approximation, and the transformation to the p-n center-of-mass system is ambiguous because of the Fermi motion.

In our experiment, an event was taken as belonging to the charge exchange reaction when the neutron momentum was higher than that of both protons in the deuteron rest system.

This definition provides a good separation of the charge exchange and charge retention channel events for the values of the four-momentum transfer from the proton to the neutron lower than about 0.6 $(GeV)^2$ (see fig. 1).

According to the above criterion, 1441 charge exchange events were found out of 8358 deuteron break-up events. The corresponding cross sections are given in table 1.

Table 1

Reaction		Cross section (mb)
$pd \to npp$	charge exchange	6.4 ± 0.2
$pd \to npp$	total	37.2± 1.4
$pd \to$ total	total(ref./4/)	82.889 ± 0.063

4. Differential Cross Section for the $pd \to npp$ Reaction

The experimental $\frac{d\sigma}{dt}$ distribution (t is the four-momentum transfer from the neutron to the proton) is shown in fig. 2. Curves A and C represent the Glauber model prediction calculated neglecting the spin dependence with the formula given by Glauber and Franco /10/. Because of insufficient experimental information on the charge exchange elementary amplitude, the amplitude for the

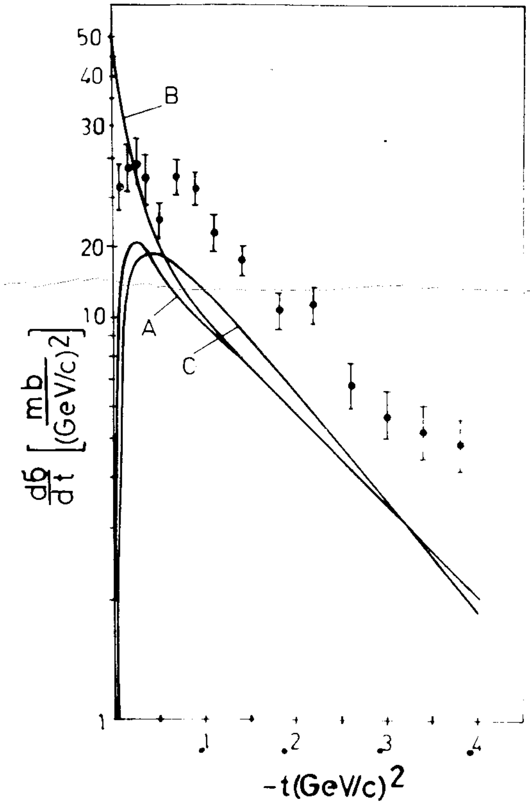

Fig. 2. The $d\sigma/dt$ distribution for charge exchange events. Curves A and C represent the Glauber model prediction according to ref. /10/. The elementary $pn \to np$ amplitude was taken in the form of $A_1 e^{b_1 t} + i A_2 e^{b_2 t}$ with A_1 , A_2 , b_1 , b_2 values fitted to the experimental data of Shepard et al. /12/ - curve A and Bizard et al. /13/ - curve C. The normalization is absolute. Curve B corresponds to the elementary charge exchange reaction with the above amplitude fitted to the experimental data of Shepard et al. (see text).

elementary charge exchange process was taken in the following simple form:

$$f_{ch.ex} = A_1 \exp(b_1 t) + i A_2 \exp(b_2 t).$$

The first term (with a greater slope) corresponds to the peripheral proton-neutron interaction via the π-exchange and is taken to be real according to ref. [11].

The experimental data by Shepard et al.[12] and Bizard et al.[13] were used in fitting the A_1, A_2, b_1 and b_2 parameters. The results from ref.[12] and [13] differ significantly hence they were fitted independently and the two sets of parameters presented in table 2 were obtained:

Table 2

Experimental data	A_1	A_2	b_1	b_2
P.F.Shepard et al.[12]	5.54±0.13	4.12±0.12	26.6±3.6	2.64±0.15
G.Bizard et al.[13]	5.18±0.06	4.90±0.05	78.0±4.9	3.25±0.10

The differential cross section for the reaction $pd \to npp$ was computed using the form-factor obtained by Alberi, Bertocchi and Bialkowski [14] from the Bressel-Kerman deuteron wave function. In fig. 2 the data of this experiment are compared with the calculations based on the parameters presented in table 2.

Curves A and C are based on the elementary data of ref. [12] and ref. [13], respectively. The influence of the deuteron effects on the $\frac{d\sigma}{dt}$ distribution can be visualized by comparing curves A and B. The last one gives the prediction based on the results of Shepard et al. [12] for the elementary $pn \to np$ differential cross-section. For $|t| > 0.15$ $(GeV/c)^2$ the influence of the deuteron effects is rather negligible in comparison with the experimental errors, but neither curve A nor C reflect properly the experimental distribution. Even for high $|t|$ values the agreement is not good. The experimental points lie systematically higher. The possible normalization error quoted in refs. [12] and [13], where the elementary data were taken from, is of the order of a few percent. This does not explain the observed difference.

The possiblity that a part of our sample results from the interactions where the inelastic intermediate state occurs may explain only a small part of the effect.

5. What We Can Learn about the Elementary Amplitude from the Deuteron Charge Exchange Reaction

A study of the deuteron break-up reaction with charge exchange at small momentum transfers can give some information on the spin structure of the elementary amplitude for the $pn \to np$ process.

The initial deuteron state is an S-state, and for low momentum transfers to the struck nucleon the final two protons are not allowed to remain in their state unless the spin-dependent interaction accurs. The contribution of the spin-dependent elementary amplitude reveals the spatial symmetry of the wave function of the two final protons [5-9]. In the framework of the impulse model and using the closure approximation, the charge exchange differential cross section is written as

$$\frac{d\sigma}{dt} = (1-S(t))\left(\frac{d\sigma}{dt}\right)_1^{el} + \left(1-\frac{1}{3}S(t)\right)\left(\frac{d\sigma}{dt}\right)_2^{el}, \qquad (2)$$

where

$$\left(\frac{d\sigma}{dt}\right)_1^{el} = \frac{\pi}{p^2}\left(|a|^2+|c|^2\right)$$

$$\left(\frac{d\sigma}{dt}\right)_2^{el} = \frac{\pi}{p^2}\left(|b|^2+|c|^2+|e|^2+|f|^2\right)$$

S denotes the deuteron form factor; the coefficients a, b, c, e, f are attached to spin invariants of the elementary charge exchange amplitude

$$M = a + b(\bar\sigma\bar n)(\bar\sigma_i\bar n) + c[(\bar\sigma\bar n)+(\bar\sigma_i\bar n)] + e(\bar\sigma\bar m)(\bar\sigma_i\bar m) + f[\bar\sigma\bar\ell](\bar\sigma_i\bar\ell).$$

The operators $\bar{\sigma}$ and $\bar{\sigma}_i$ correspond to the fast particle and the i -th nucleon in the deuteron. The scalar forward scattering amplitudes in the helicity representation are written as

$$a = \frac{1}{2}(f_{++,++} + f_{+-,+-})$$

$$b = e = \frac{1}{2} f_{++,--}$$

$$c = 0$$

$$f = \frac{1}{2}(f_{+-,+-} - f_{++,++})$$

It is worth noting that even if the spin-flip amplitude vanishes, a spatially symmetrical state of two final protons can appear while $f \neq 0$.

For the forward scattering one obtaines:

$$\left(\frac{d\sigma}{dt}\right)_1^{e\ell} = \frac{\pi}{p^2}|a|^2, \quad \left(\frac{d\sigma}{dt}\right)_2^{e\ell} = \frac{\pi}{p^2}(2|b|^2 + |f|^2).$$

The contribution of the spin-dependent amplitude has been estimated assuming the following parametrization

$$\left(\frac{d\sigma}{dt}\right)_2^{e\ell} = x_1 e^{b_1 t} + x_2 e^{b_2 t},$$

where

$$\left(\frac{d\sigma}{dt}\right)_1^{e\ell} = \left(\frac{d\sigma}{dt}\right)^{e\ell} - \left(\frac{d\sigma}{dt}\right)_2^{e\ell}.$$

The parameters x_1 and x_2 have been obtained by fitting formula (2) to the experimental $\left(\frac{d\sigma}{dt}\right)_d^{ch.ex.}$ distribution. The results are the following:

1. $x_1 = 7.0 \pm 4.4$, $x_2 = 0.07 \pm 0.6$ for the elementary amplitude fitted to the data of ref. /12/ ,
2. $x_1 = 16.7 \pm 16.7$, $x_2 = 5.2 \pm 7.1$ for the elementary amplitude fitted to the data of ref. /13/.

The curves calculated according to formula (2) with the above parametrization were normalized to the experimental distribution in the $|t| > 0.15$ $(GeV/c)^2$ region (fig. 3).

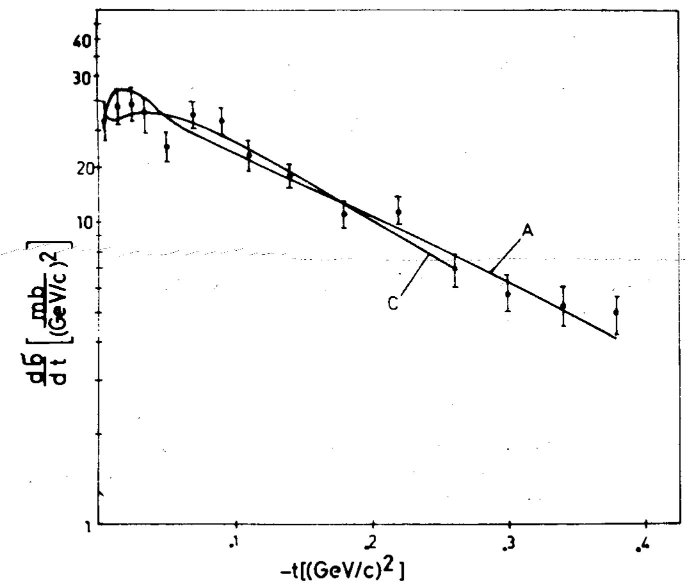

Fig. 3. The $d\sigma/dt$ distribution for charge-exchange events. Curves A and C were calculated taking into account the contribution of the spin-independent part in the amplitude, according to formula (2), and normalized to the experimental distribution in the $|t| > 0.15$ $(GeV/c)^2$ region.

Using the above x_1 and x_2 values one obtains the contribution of the spin-independent amplitude

$$R = \frac{\left(\frac{d\sigma}{dt}\right)_1^{e\ell}}{\left(\frac{d\sigma}{dt}\right)_1^{e\ell} + \left(\frac{d\sigma}{dt}\right)_2^{e\ell}}\Bigg|_{t=0} = \frac{|a|^2}{|a|^2 + 2|b|^2 + |f|^2}\Bigg|_{t=0}$$

equal to

1. $R = 0.86 \pm 0.09$
2. $R = 0.57 \pm 0.22$

for elementary amplitude fitted to refs. /12/ and /13/ , respectively.

It should be pointed out that, when statistics are increased, a more subtle treatment should be applied taking into account the double scattering effects, the final state interaction and the occurence of the inelastic intermediate states. The influence of the double scattering on R, according to ref. /8/, may diminish the value of R by about 30%.

6. Momentum and Angular Distribution of the Spectator Particle

We define as a spectaror the slowest nucleon in the event. One should note that the above definition is adequate the physical meaning of the spectator if the other nucleon is distinctly faster.

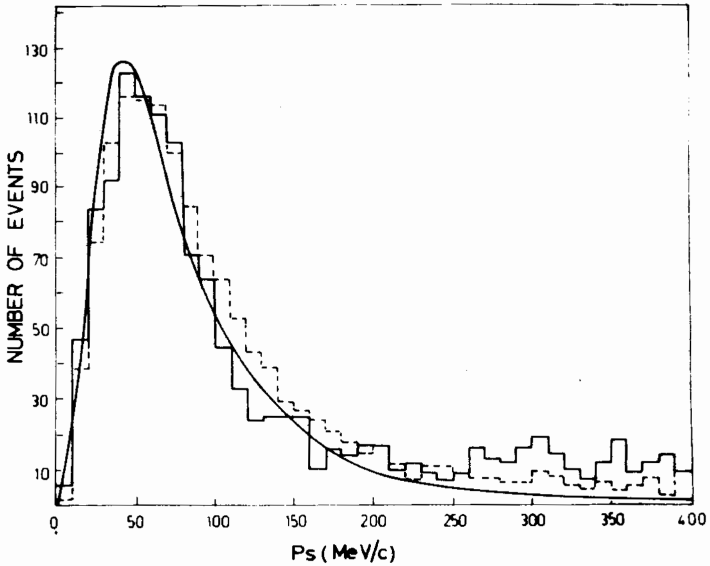

Fig. 4. The experimental distribution of the spectator nucleon momentum. The dashed histogram represents the events from the charge-retention channel and is normalized to the full-line histogram in the $p_s < 100$ MeV/c region. The curve represents the Gartenhaus-Moravcsik wave function of the deuteron.

In fig. 4 the experimental distribution of the spectator momentum is compared with the Gartenhaus-Moravcsik wave function

$$\Psi_0(q) = \sum_i F_i \exp(-f_i q^2) \qquad \Psi_2(q) = q^2 \sum_i G_i \exp(-g_i q^2)$$

calculated with the parameter values listed in table 3 (taken from ref. /15/).

Table 3

	$F_i\,(\mathrm{GeV/c})^{-3/2}$	$f_i\,(\mathrm{GeV/c})^{-2}$	$G_i\,(\mathrm{GeV/c})^{-7/2}$	$g_i\,(\mathrm{GeV/c})^{-2}$
1	4.9965	2034.129	4.2061	7.925
2	24.3705	408.220	30.3101	28.461
3	9.4082	87.934	15.1201	111.632
4	2.1399	21.495	106.8280	99.161
5.	-0.06246	1.702	266.3585	388.459

For about $(27 \pm 1)\%$ of events the spectator momentum exceeds 200 MeV/c, i.e., considerably more than any wave function predicts (e.g., about 8% in the case of the G – M wave function). In the charge retention channel (i.e., the break-up without charge exchange) the corresponding number is $(16 \pm 1)\%$ so the effect seems to be channel-dependent.

The angular distribution of the slowest proton in the charge exchange reaction is almost isotropic for different spectator momentum intervals (fig. 5 a,b,c). In the charge retention channel the spectator angular distribution for $p_s > 80$ MeV/c exhibits a significant deviation from isotropy. It seems, however, that the observed isotropy in the charge exchange channel may be due to the compensation caused by three different factors. The influence of the final state interaction and the flux factor enrich the number of the spectator emitted in the forward direction whereas the strong momentum dependence of the charge exchange cross section produces an opposite effect.

As will be shown below, the interference between the

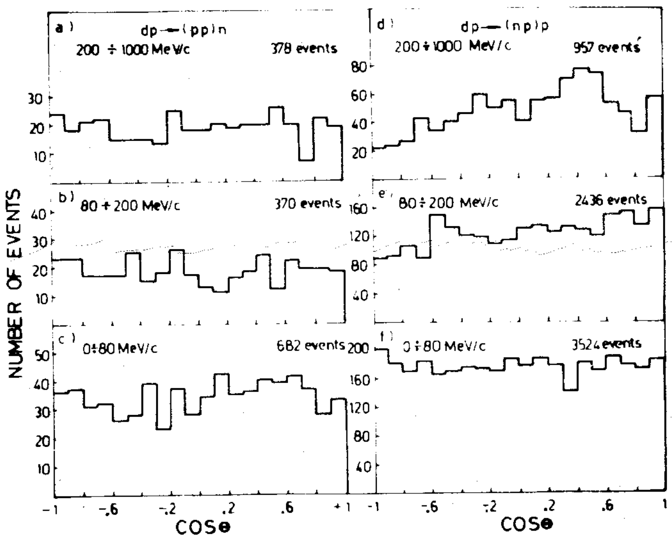

Fig. 5. The angular distributions of the spectator nucleon for different spectator momentum intervals for the charge-exchange (a, b, c) and charge retention (d.e.f) channels.

spectator and the struck nucleon cannot explain the excess of high momentum spectators. The symmetrization effects may play an important role for high spectator momenta and for low four-momentum transfers. The momentum distribution of the slowest particle for low momentum transfer ($|t| < 0.06\ (GeV/c)^2$) is shown in fig. 6. For comparison the momentum distribution for the charge retention channel is also given (solid line histogram). The significant difference for $p_s > 100$ MeV/c is observed in comparison with the direct channel. The difference may be explained by the fact that in the charge exchange channel the antisymmetrical part of the two-proton spatial wave function dominates. For high t -values the momentum of the struck particle becomes higher and therefore the symmetrization effects suppress higher momenta of spectators. Hence, the observed excess of the high-momentum spectators ($p_s > 200$ MeV/c) in the

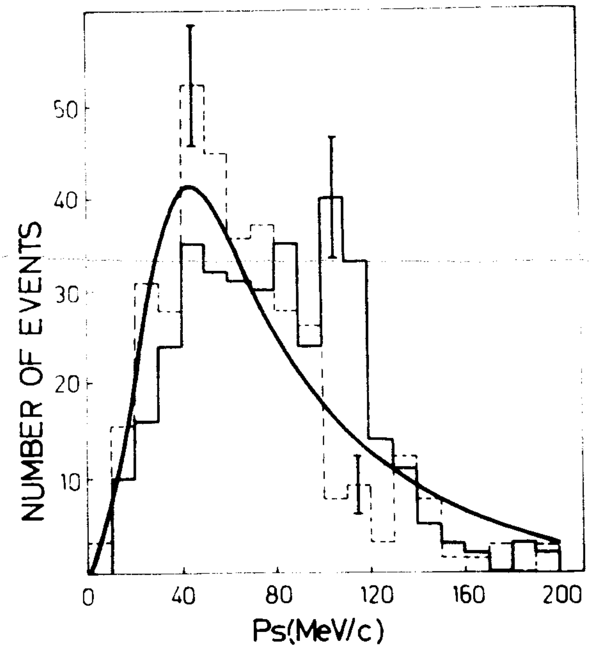

Fig. 6. The momentum distribution of the spectator particle in the $|t| < 0.06\ (GeV/c)^2$ region for the charge-exchange (broken line) and charge retention (full line) channels. The curve represents Gartenhaus-Moravcsik wave function predictions. The curve and histograms are normalized in the $p_s < 200\ (MeV/c)^2$ region.

charge exchange channel cannot be explained by the interference effect.

7. Discussion of the Mechanisms Different from the Single Scattering

It is well-known that the processes involving both the nucleons from the deuteron (e.g., FSI, double scattering of the incident proton) amount to several percent of the total cross section. Nevertheless, one might expect that in certain kinematic regions they will be

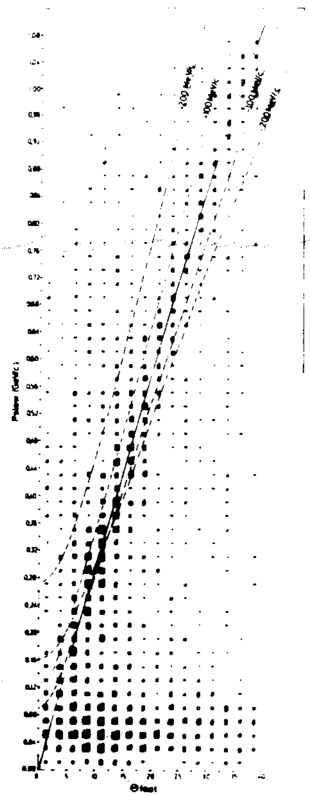

Fig. 7. The neutron scattering angle versus a proton momentum. One event is represented by two points. The full curve corresponds to the elastic NN kinematics. The broken lines represent the elastic NN kinematics calculations with the Fermi momentum of the target taken into account.

more pronounced. In order to analyze them, let us examine the scatter plot presented in fig. 7 where the neutron scattering angles versus the proton momenta are plotted (one event is represented by two points corresponding to two protons). Two regions populated by the majority of the events are clearly seen: one corresponds to low momenta of the spectators, another one to the kinematics of the elastic scattering of protons

on the free nucleon from the deuteron. The dispersion of points around the solid line is due to the Fermi momentum, the spread of the beam momentum and the measurement errors. To display the influence of the Fermi motion of nucleons on the population of points, the curves corresponding to a single scattering on nucleons with different Fermi momenta parallel to the beam direction are also shown in the figure.* There are still several percent of the events out of the region lying between the curves corresponding to the parallel components of the spectator momenta equal to ±200 MeV/c (see the figure).

The events with spectator momenta less than 200 MeV/c are consistent with the assumption that the single scattering occurs.

It seems that the different mechanisms are responsible for the remaining events (with p_s > 200 MeV/c) which lie below and above the curve correspoding to the elastic nucleon-nucleon scattering. We call them A-class and B-class, respectively.

7.1. A-class

For the fixed scattering angle of the fast particle the most probable momentum transferred in the double scattering is equal to one half the momentum of the particle involved in the single scattering /17/. The majority of the events correspoding to the double scattering lies at least for large scattering angles below the curve (solid line in fig. 7) representing the elastic scattering and therefore contributes mainly to the discussed class of the events.

---

* The curves were calculated assuming that during a collision the spectator nucleon is on the mass shell. The energy conservation was assured by taking lower mass m_t of the target nucleon according to the formula:

$$M_d = \sqrt{m_N^2 + p_F^2} + \sqrt{m_t^2 + p_F^2},$$

where M_d is the deuteron mass and p_F is the Fermi momentum of the nucleon.

For the events, attributed to class A, the momentum and angular distributions of the slowest nucleon are shown in figs. 11b, 12b.

In the distribution of the relative angle of the two protons the lack of large relative angles is observed; all the events are accumulated in a $(-0.4 \div 1)\ \cos\phi(p_1, p_2)$ interval.

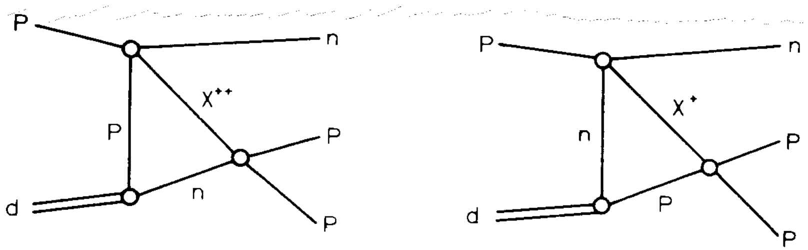

Fig. 8. Graphs involving the intermediate isobar X-state.

7.2. B-class

It seems that a part of the events attributed to class B corresponds to the production and absorption of the intermediate isobar state according to the diagrams shown in fig. 8.

The following observations may support this hypothesis:

a) On the scatter plot presented in fig. 9 these events are situated in the neighbourhood of the curve corresponding to the $NN \to XN$ scattering. The X-particle has a mass larger than the nucleon mass. The curves calculated for M_X equal to 1150 and 1236 MeV are also shown.

b) The distribution of M_X is shown in fig. 10. The mass of the X particle was calculated assuming the two-body kinematics in the upper vertex of the graphs presented in fig. 8. The Fermi motion was neglected in the calculations. The width of the M_X distribution for $P_s < 200$ MeV/c centered at the nucleon mass value (fig. 10a) reflects the spread of the distribution introduced by the Fermi motion and by the experimental resolution.

It is seen in fig. 10b that the M_X distribution for the B-class favours masses higher than the nucleon mass. Only one half the events may be consistent with the assumption that the $\Delta(1236)$ is produced in the intermediate state.

c) The average momentum of the slowest particle

Fig. 9. The distribution of the scattering angle of the neutron vs. its momentum. Description of the curves as for fig. 7.

about 400 MeV/c (see fig. 11a) and the majority of particles are moving backwards (see fig. 12a).

d) The two protons are emitted predominantly in the opposite directions (fig. 13, full line histogram).

These features of the process are natural if one takes into account that:

a) The final state interaction plays an important role for the low relative momenta of the nucleon and the X -particle.

b) The incident momentum of the nucleon involved in

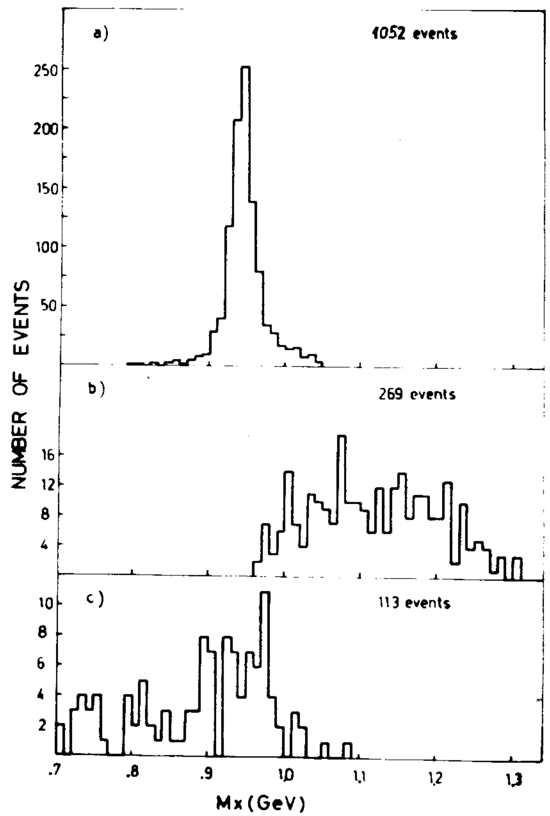

Fig. 10. The distribution of M_X calculated on the assumption of the two body kinematics in the upper vertex of the graphs in fig. 8 for events from different classes .

the final state interaction is low and consequently provides a low CMS momentum of the XN system.

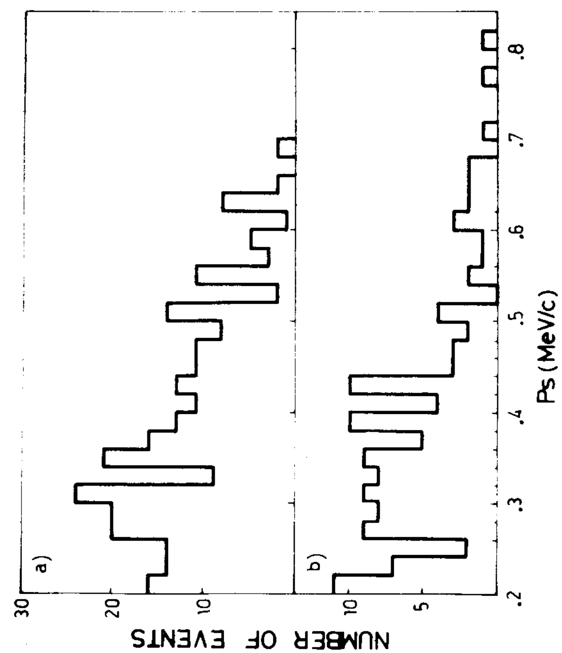

Fig. 11. The distributions of the spectator particle momentum for events from classes B(a) and A(b).

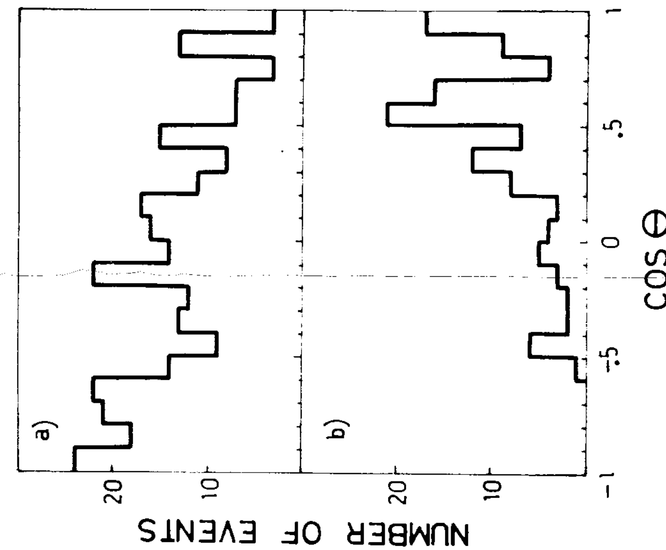

Fig. 12. The angular distributions of the spectator proton for classes B(a) and A(b).

c) The X particle with large mass is emitted forwards.

Summarizing, we can say that our samples may be ascribed to the different reaction mechanisms:

The events with the spectator momentum $p_s < 200$ MeV/c, representing about 73% of the total sample, correspond mainly to the single scattering process. Because of the

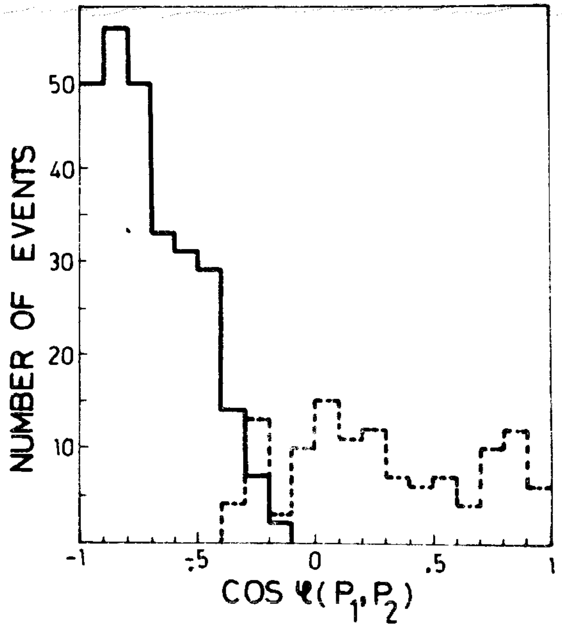

Fig. 13. The distribution of the relative angle between two protons in the deuteron rest frame for classes B (full line) and A (dashed line).

cut in the spectator momentum distribution one can expect that about 8% of the single scattering interactions are still present in the A and B classes.

Class A (about 8% of the total sample) contains, apart to the single scattering interactions, the events corresponding to the double scattering and the nucleon-nucleon final state interaction.

For explaining the occurence of a part of the events in the B -class (about 19% of the total sample) the hypothesis of the existence of the intermediate isobar may be helpful.

8. Conclusions

In the present work we have studied the charge exchange process in the $dp \to npp$ reaction at the 3.3 GeV/c incident deuteron momentum. The sample containing 1441 events was analysed.

It is shown that the use of the deuteron beam leads to a distinct selection of the $dp \to npp$ charge exchange channel with small losses and contaminations.

Although lack of precise experimental data on the elementary nucleon-nucleon interactions in the considered energy region and the incompleteness of existing theoretical calculations restrict the possibility of quantitative conclusions, one can extract some supplementary information on the elementary charge exchange process and the $dp \to ppn$ charge exchange reaction:

1. The contribution of the spin-independent part of the amplitude in the elementary $np \to pn$ charge exchange reaction in the forward direction is estimated to be $R = 0.86 \pm 0.09$ or $R = 0.57 \pm 0.22$ if the elementary data of refs. /12/ and /13/ are used, respectively.

2. A part of events cannot be described by the spectator model. The final state interaction of slow nucleons and the double scattering of the fast incoming nucleon cannot be responsible for all events inconsistent with the spectator mode. It is suggested that a part of these events may be due to the production of the intermediate $\Delta_{3/2,3/2}$ state.

We are greatly indebted to our measuring staff for careful measurements, to JINR proton sunchrotron and the 1 HBC crews for excellent performance of the accelerator and the chamber.

We also thank Professor G.Bialkowski and Dr. M.Swiecki for valuable discussion and remarks.

References

1. B.Musgrave. Proc. of CALTECH Conf. on Phenomenology in Particle Physics, ed. California Inst. of Tech., p. 467 (1971).
2. J.Saudinos , C.Wilkin. Ann. Rev. of Nucl.Sc., 24 (1974).
3. B.S.Aladashvili et al. JINR, 1-7645, Dubna, 1973.
4. D.V.Bugg et al. Phys.Rev., 146, 980 (1966).
5. I.J.Pomeranchuk. DAN SSSR, 78, 246 (1951).
6. L.I.Lapidus. ZETF, 32, 1437 (1957).
7. B.M.Schwartzschild. UCRL report - 17572 (1967).
8. G.I.Lykasov, A.V.Tarasov. JINR, P2-7324, Dubna, 1973.
9. N.W.Dean. Phys.Rev., 5D, 1662 (1972). Phys.Rev., 5D, 2832 (1972).
10. R.J.Glauber, V.Franco. Phys.Rev., 156, 1685 (1967).
11. N.Byers. Phys.Rev., 156, 1703 (1967).
12. P.F.Shepard et al. Princeton-Pennsylvania Accelerator Report PPAR-10 (1969).
13. G.Bizard et al. Submitted paper, II-nd International Conference on Elementary Particles, Aix-en-Provence (1973).
14. G.Alberi, L.Bertocchi, G.Bialkowski. Nucl.Phys., B17, 621 (1970).
15. G.Alberi. INEN Report, INEN/AE-73/1.
16. N.W.Dean. Phys.Rev.Lett., 27, 276 (1971).
17. F.Bradamante et al. Nucl.Phys., B28, 349 (1971).

Received by Publishing Department
on July 11, 1974.